Porous Glasses, Binary Glasses, and Composite Glasses from Aerogels

Thierry Woignier, Jérôme Reynes, Jean Phalippou

Porous Glasses, Binary Glasses and Composite Glasses from Aerogels

Thierry Woignier[a*,b,1], Jerome Reynes[c,2] and Jean Phalippou[c,3]

[a] Aix Marseille Univ, Univ Avignon, CNRS, IRD, IMBE, Marseille, France

[b] IRD UMR 237-Campus Agro Environnemental Caraïbes-B.P. 214 Petit Morne, 97232, Le Lamentin, Martinique

[c] CNRS-Université Montpellier II, Place E. Bataillon, 34095, Montpellier Cedex 5, France

[1] E-mail: woignier@imbe.fr.
[2] E-mail: reynes.jerome@neuf.fr.
[3] E-mail: jean.phalippou698@orange.fr.

Abstract
This chapter describes the different steps of the transformations of a gel into an aerogel and into glass and the physical properties of the different materials derived from sintered silica aerogels. Silica glasses can be synthesized by sintering silica aerogels at temperatures ranging from 900 to 1,200 °C close to half the temperatures used for the glass melting process. The heat treatment can be taillored to obtain fully densified or porous glasses. Supercritical drying also enables the synthesis of aerogels from a wide range of binary compositions giving rise to binary or ternary silicate glasses after sintering. Another interesting application of aerogels is as a host matrix for the synthesis of multi-phase materials, doped material glasses, or composites. Their large pore volume is used as a sponge to incorporate chemical species in such a way as to form a two-phase material. The chemical species are first processed in liquid form and can be dried after the pores are filled. The result is a nanocomposite material composed of salt oxide embedded in the silica matrix.

Keywords: Aerogels, sintering , porous glasses, composites glasses, nuclear wastes.

1. Introduction

The physical and chemical properties of conventional glasses have been studied for many years and their applications are well known. Glasses are traditionally used in optical materials and containers and also as fibers for mechanical reinforcement as well as “exotic” applications such as the storage of nuclear waste [1–3].

In recent decades, a new kind of glass synthesis has been extensively described in the literature. These glasses are no longer prepared using standard melting and refining processes but by a sol-gel method [4]. The structure of these materials results from the aggregation of colloidal oxide building blocks such as SiO_2, Al_2O_3, ZrO_2, B_2O_3, TiO_2. The structure formation mechanism does not allow the entire space to be filled, resulting

M.A. Aegerter et al. (eds.), *Aerogels Handbook*, Advances in Sol-Gel Derived Materials and Technologies, DOI 10.1007/978-1-4419-7589-8_5,

in a porous amorphous material. These gels are transformed into aerogels by supercritical drying, and a further sintering step collapses the porosity to a controllable degree [5, 6].

This chapter deals with glasses, porous glasses and composite glasses derived from sintered silica aerogels.

In part 2, we explain the avantages of this new method of synthetizing glasses and introduce the main steps of the sol-gel-glass process.

In part 3, we describe how sintering the viscous flow transforms the aerogel into glass. We present the sintering model proposed by Scherer and characterize the structural transformations using scattering techniques.

In part 4, we give examples of porous glasses, multicomponenst glasses and nanocomposites glasses obtained from aerogels and the different ways to synthesize these materials. We discuss the advantages of using composite aerogel as precursors (host matrix), focusing on a specific application: containment of radioactives wastes.

2. Glasses obtained using the sol-gel process

Thirty years ago "sol-gel processes" were shown to be a new way to synthesize materials as different as ceramics, glasses, or composites. Brinker and Scherer [4] demonstrated the potential of this technique for the synthesis of materials in the form of films, fibers, or bulk products.

The standard procedure for making glasses includes a high temperature step that ensures the raw materials have fused at the molecular level; the liquid amorphous structure is preserved by rapid cooling of the melt. In a sol-gel process, this high temperature step is omitted. Homogenization is achieved in solution at room temperature and particle cross-linking and preservation of the amorphous structure are accomplished by the gelation step. Further heat treatments only serve to remove organic species and hydroxyls, and to eliminate porosity and to induce crystallization, if required [4,6]. The sol-gel process has several unique flexible features that are of great importance in preparing pure homogeneous glasses: (1) the high purity of the starting compounds that can be preserved during the process; (2) for multicomponent systems, rapid homogenization of the different chemical species can be achieved at the molecular level in the solution using chemical reactions; (3) in the case of compositions leading to a glass, the gel is amorphous and can be transformed into glass without melting or refining. The sintering treatment is carried out at temperatures (in °C) one-third to one-half lower than those required to melt the glass forming components; (4) the morphology of the product, film, fiber, and bulk materials can be controlled by adjusting viscosity at room temperature; (5) the large pore volume of the gel can be used as a host matrix for other chemical species by means of impregnation.

The challenge is obtaining a solid, dense, mineral, amorphous material from a liquid solution, which is generally organic. Several transformations of the gelling solution are necessary [4,6]. The first step is forming a gel from the solution. There are two standard ways to obtain silica-based gels [7]: destabilization of silica sols or hydrolysis and polycondensation reactions of an organometallic compound of silicon [7]. Both methods result in noncrystalline materials containing substantial amounts of water and organic liquids, but both can be eliminated through suitable drying treatments. The drying process can be carried out at ambient temperature but considerable shrinkage occurs, which turns

the soft wet gel into several pieces of solid material, with no control possible over the size, morphology, or porous properties of the dried samples. Supercritical drying is one way to avoid these problems. After this process, the aerogel is a solid, amorphous but extremely porous material (75–99% porosity). The last step of the transformation is a densification treatment to convert the aerogels into solid glasses devoid of porosity by sintering.

Small-angle scattering techniques (X-ray or neutron scattering) provide information on the structure and compactness of the clusters that form the gel network. The aerogel network is often described as an assembly of clusters (~50 nm). The clusters can be fractal ($Df \sim 2$), i.e. built by aggregation of small particles (~1–2 nm) [7–10]. This 3D network is completely open and the pore sizes range from micro to macroporosity. Although the aerogel networks are rather different from the structure of silica glasses, Raman, infrared, and NMR spectroscopy used to characterize the molecular structure revealed identical signatures to those observed in vitreous silica [11].

These kinds of porous materials can be considered as porous glasses even though they differ in the way they reach the "glassy" state

3 Sintering of aerogels.

Thermal treatments enable the conversion of the aerogel into porous glass and /or fully densified silica glass. The final density of the sintered aerogels will depend on the thermal treatment applied. Sintering is a process by which the surface area of a material is decreased by mass transport. For amorphous materials, viscous flow is important because it is much faster than any competing densification process resulting from diffusion. The rate of viscous sintering is calculated using the energy balance concept proposed by Frenkel [12]: the energy dissipated in a viscous flow is equal to the energy liberated by the reduction in surface area; therefore, at a given density, a body with smaller pores densifies more rapidly.

Aerogels provide a stringent test of sintering theories [13-15], because they can be prepared at low densities, so changes in density, pore size, and surface area can be monitored over a wide range (16].

3.1. Sintering by viscous flow: the cylinder model

The isothermal densification kinetics of aerogels have been found to fit the Scherer' model (cylinder model) [6,17,18], with viscosity as the only fitting parameter. This model describes viscous flow sintering of amorphous material over a wide range of porosity (0–95%). The porous material under analysis is considered as a cubic array of cylinders. The length of the cylinders is ℓ and the radius r. Sintering by viscous flow leads to shrinkage in length while the radius increases. The relative density $\rho_r = \rho/\rho_s$ where ρ is the bulk density and ρ_s the skeletal density is plotted as a function of a reduced time:

$$K\,(t - t_0) \qquad (1)$$

where t is the sintering time, t_0 is a fictitious time, and K is a constant at a given temperature:

$$K = \gamma / \eta \, \ell_i \, (\rho_s/\rho_i)^{1/3} \qquad (2)$$

where γ is the surface energy and η the viscosity. ℓ_i and ρ_i refer to the length of the cell and to the initial bulk density of the aerogel, respectively.

Onorato studied the sintering kinetics of silica aerogels [18] isothermally and at a constant heating rate, and found good agreement with the cylinder model in both cases. In the same study it was shown that the atmosphere has a marked effect on the densification rate, which is faster in air than in oxygen, whereas in chlorine, the rate was slower because of the removal of OH.

In the study reported in this chapter, dilatometric measurements performed at several temperatures ranging from 1,005 °C to 1,250 °C as a function of time, provided evidence that sintering occurs through viscous flow.

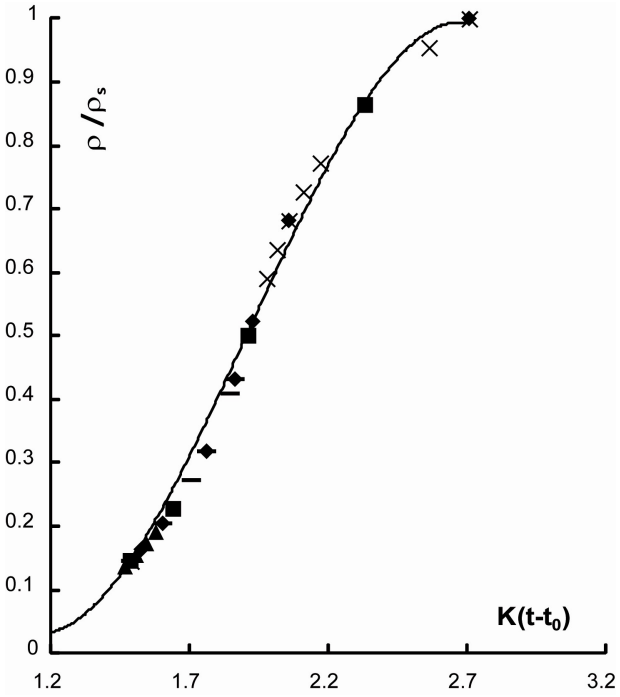

Fig. 1 Plot of relative density ρ_a/ρ_s versus reduced time for a base-catalyzed silica aerogel treated at different temperatures: ▲1,000 °C, — 1,050 °C, ♦ 1,100 °C, ■ 1,200 °C, x 1,250 °C. The line corresponds to Scherer's theoretical model.

Figure 1 shows that Scherer's model fits data on aerogels obtained in five isothermal sintering treatments. The activation energy associated with viscosity and estimated from sintering measurements was close to 370 kJ/mole. This is lower than for a

silica glass with a hydroxyl content of 1,300 ppm, which is about 500 kJ/mole. The value of the activation energy depends on the atmosphere but also on hydroxyl content. In the present study, the hydroxyl content of the silica glass obtained from sintered aerogel ranged from 3,000 to 5,000 ppm.
Water content plays an important role in sintering kinetics. Reducing the water content increases the sintering temperature range. When the samples have a high water content, foaming phenomenon occurs during sintering (figure 2). Bubbles are due to water molecules that first appear in the core of the sample. During sintering, the first open pores to close are those located at the surface. More water molecules and air are trapped in the solid core network, which is not totally densified. The bubbles grow and tend to expand with an increase in temperature.

Figure 2. Aerogels after sintering and foaming effect

To reduce the water content, a dehydration treatment is performed during sintering using gases such as CCl_4, Cl_2, or F_2 [6] .

3.2 Changes in texture

Silica aerogels are generally fractal objects [8–10]. Changes in the texture of aerogels with sintering is usually described using specific surface area, porous features (porosity, mean pore size distribution), or solid-phase microstructure (fractal dimension, cluster, and primary particle sizes). Aerogels are composed of primary particles 1-2 nm in size. These particles aggregate to form clusters that stick together and create a homogeneous particle network. The cluster exhibits a fractal geometry as evidenced by small-angle X-ray scattering [10,19]. The fractal domain stretches between the correlation length ξ and the particle size a. The correlation length corresponds to the size of the fractal cluster. The fractal dimension is directly measured by the slope of the curve log $I(q)$ versus log q. To monitor changes in the texture of the aerogel during sintering, the transformation of the fractal clusters can be characterized. Small angle scattering of X-rays (SAXS) and

neutrons (SANS) has been used to monitor structural changes in aerogels during sintering. The data showed an increase in the primary particle size and a decrease in the correlation length, while the fractal dimension remained unchanged [6,19]. Schaefer et al. [20] used neutron spin echo (NSE) spectroscopy and demonstrated an increase in short-range connectivity (i.e., at a length scale ≤ 100 nm) in the network upon heating.

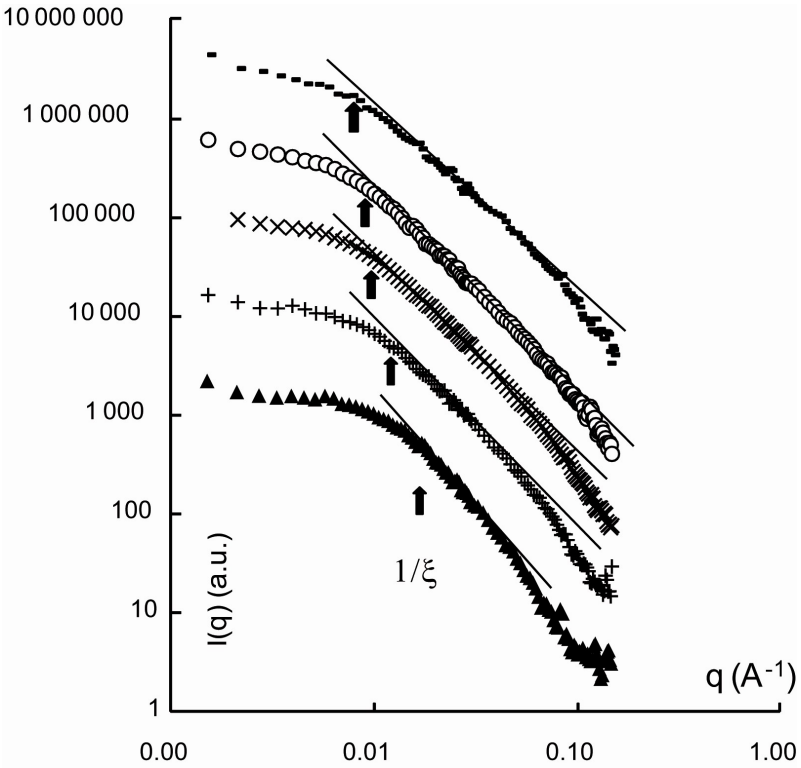

Fig. 3. SAXS measurements obtained for a series of fractal partially densified aerogels. 0.16 gcm^{-3}(—), 0.29 gcm^{-3}(●), 0.33 gcm^{-3}(x), 0.47 gcm^{-3}(+), 0.72 gcm^{-3}(▲).
The sintering treatment was performed at 1,000 °C as a function of time. ξ decreased (see arrows in the top panel), the slope (fractal dimension) is shown to guide the eye. Adapted from [13]

In the study described in this chapter, the sintering of fractal aerogels was analyzed as a function of density for an isothermal treatment performed at 1,000 °C in air. The fractal dimension *Df* did not change significantly during the first stages of sintering about 2.2–2.3. However, as shown in Fig. 3, there was a decrease in the correlation length with an increase in the particle size. Changes in ξ and *a* with sintering showed that at the beginning of sintering the size of the clusters and of the particles changed in opposite ways: ξ decreased and *a* increased. In the last step, the fractal dimension increased as sintering proceeded. All these results are consistent with

expectations, since densification occurs initially at the smallest length scale; ξ decreases as a consequence of densification of the local structure, which causes a uniform contraction. This behavior was also estimated theoretically from a scaling model describing fractal geometry [21]

4 Glasses derived from aerogels

4.1 Porous glasses

Thanks to the viscosity resulting from sintering it is possible to progressively collapse the porosity of the aerogel and to control the amplitude of the collapse by modifying the duration of the heat treatment at 1,000°C (Figure 4).

These curves are obviously strongly dependent on the temperature of the heat treatment but also on the hydroxyl content of the aerogel, which affects the viscosity of the aerogel [6].

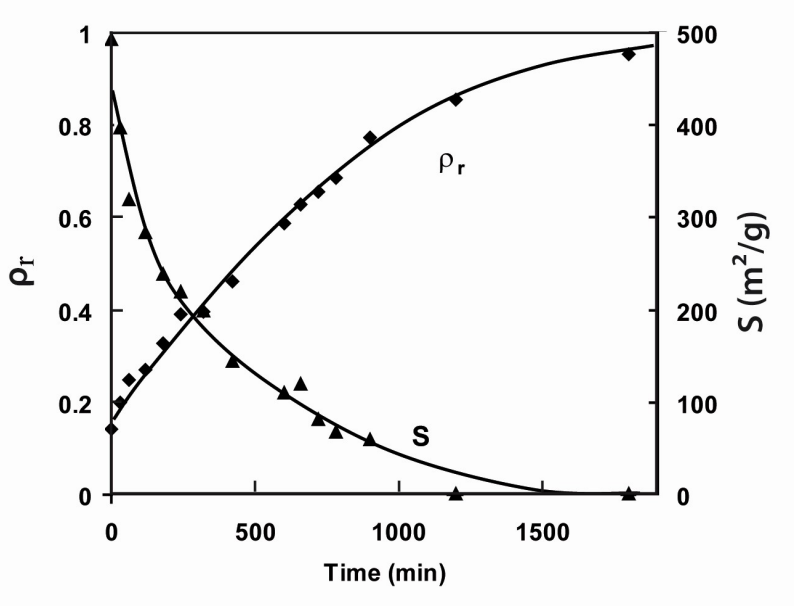

Figure 4. Changes in aerogel relative density ρ_r (black squares) and specific surface area S (black triangles) versus sintering time at 1,000 °C.

Gels that are originally noncrystalline may crystallize during a subsequent heat treatment. The successful formation of a glass is the result of competition between the phenomena that lead to densification and those that cause crystallization [22]. Figure 5 shows the different steps of sintering between the aerogel sample on the left and the sample on the right, which is an aerogel densified glass obtained by sintering (the aerogel densified glass has been polished)

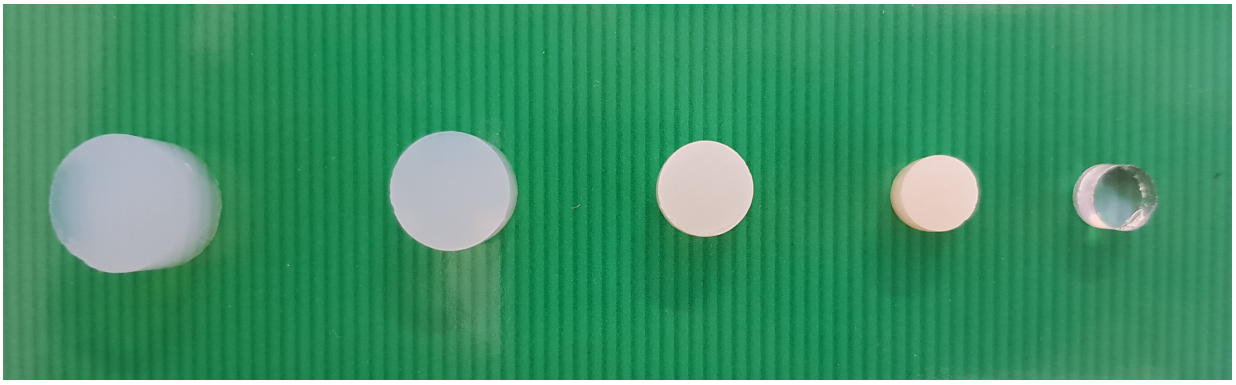

Figure 5. Set of partially sintered aerogels: from an aerogel (ρ is 0.3 g.cm^{-3}, sample on the left) to a fully sintered aerogel (transparent silica glass on the right, ρ is 2.2 g.cm^{-3}).

Figure 4 shows that it is possible to control both the pore volume and the relative density of the partially sintered aerogels between 0.3 g.cm^{-3}and 2.2 g.cm^{-3}. Controlling the density of these porous glasses also enables control of the physical properties that depend directly on density and pore size, including the elastic modulus, mechanical resistance, optical features (transparency, refractive index), and permeability.

Table 1 lists some of the physical properties of standard aerogel (ρ_a = 0.3 g.cm^{-3}) and the fully sintered aerogels (ρ_a = 2.2 g.cm^{-3}). The table shows the remarkable changes in the physical properties of the partially sintered aerogels that can be obtained by controlled sintering.

Table 1. Bulk density (ρ_a), pore volume (P), specific surface area (S), refractive index (n_d), Young's modulus (E) , flexural strength (σ) and Vickers hardness (Hv).

	ρ (g.cm^{-3})	P (%)	S (m^{2}g^{-1})	n_d	E (Pa)	σ (Pa)	Hv (kg.mm^{-2})
Aerogel	0.3	85	410	1.02	1 10^8	5 10^5	1
Sintered aerogel	2.2	0	≈ 0	1.458	7.3 10^{10}	95 10^6	750

Since a number of physical properties including the refractive index, dielectric constant, thermal conductivity, and accoustic impedance are correlated with porosity, a material that continuously changes its density will also undergo a corresponding change in these properties. The manufacture of gradient porous glasses is thus a promising area of research. For example, it was shown that an aerogel placed in a furnace with a temperature gradient ranging from 900 to 1,150 °C gives rise to a graded porous material in which the top of the sample is fully dense while the bottom maintains 95% open porosity [23].

The fact that silica aerogels can be manufactured in large formats (i.e. monolithic panes) while remaining transparent makes silica aerogels an attractive glazing material for superinsulating windows [24]. However, monolithic aerogel panes are very brittle, their typical flexural strength varies between 1 kPa and 1 MPa, [6], making their application as window glazing materials questionable. A report in the literature [25] describes an approach to synthesize glass windows via densification of silica aerogels. Although the loss of porosity and the resulting increase in thermal conductivity are drawbacks linked to the densification process, a combination of enhanced mechanical performance and optical transparency suggests that partially sintered silica aerogels could be used as new material for window glazing. Preliminary experimental results indicated lighter weight (density 1.8 g/cm^3, compared to 2.5 g/cm^3 for float glass) and improved thermal insulation (thermal conductivity $k \approx 0.18$ W/(mK), compared to 0.92 W/(mK) for float glass. Aerogel glass materials with high visible transparency ($T_{vis} \approx 95.4\%$ at 500 nm compared to 92.0% for float glass) can be achieved by annealing an acid-catalyzed silica aerogel precursor at 700 °C [25].

Ultrasonic waves have special effects on chemical reactions, and are an alternative way to synthesize gels without using solvents [26]. These aeogels are called sono aerogels. Despite major structural differences (no fractal structure, higher bulk density, higher specific surface area, etc.) silica sono aerogels can be converted into dense silica glass using a very similar process to the one described for standard aerogels. Sono aerogels were sintered in a tube furnace in an atmosphere that changed from N_2 through 0_2 to He. The sudden change in volume began at 1,050 °C and sintering was complete at 1,100 °C, as expected [27].

4.2 Multicomponent glasses

Supercritical drying has also been used to synthesize aerogels of binary and ternary composition and led to the production of borosilicate glasses, phosphosilicate glasses, Neodymium silica glasses and complex glass ceramics containing BPO_4 or cordierite and mullite compositions [28-31].

Aerogels in the binary and ternary systems SiO_2-B_2O_3, SiO_2-P_2O_5 and SiO_2-B_2O_3-P_2O_5 were prepared and converted into glasses by sintering heat treatment [28,29]. The results showed that the range of sintering temperatures decreases with an increase in B_2O_3 content. The transformation of aerogels into glasses was achieved in the tempretaure range 800 °C-950 °C. This temperature range corresponds to viscosities of between 10^{11} and $10^{9.5}$ P. In the S_i0_2-P_2O_5 system, the sintering temperature is also affected and the pore collapse is important for temperatures in the range 1,000-1,080 °C corresponding to viscosities of around 10^{11} P. These glasses have similar properties (density, refractive index) to those obtained by melting techniques [29].

In the ternary SiO_2-B_2O_3-P_2O_5 system, X-ray diffraction spectra showed the presence of a crystalline phase: borophosphate (BPO_4) This phase is isoelectronic to silica and stable in glasses that contain both B_2O_3 and P_2O_5.

Binary titania silica glasses were prepared by densification of a titania–silica sono aerogel. Results showed that the sintering also occurred via the viscous flow mechanism [32].

Silica glasses doped with neodymium have been synthesized from aerogels [33] for laser applications. However, the dispersibility of Nd^{3+} ions in the laser glasses influences their fluorescence lifetime. Unfortunately, Nd^{3+} ions can only dissolve in the $Si0_2$ matrix in small quantities and Nd ions crystallize as Nd_20_3. Results showed that the fluorescence lifetime of 1% Nd_20_3 -99% SiO_2 glass obtained from binary aerogels is short because of clustering of Nd^{3+} and crystallization of Nd_2O_3 microcrystals. Nd-Al codoped silica glasses were prepared by sintering an aerogel with a double metal alkoxide (Al and Nd). With the addition of 3% molar Al_2O_3, Nd^{3+} ions dispersed and the fluorescent lifetime increased significantly. However, it should be noted that with high concentrations of Nd and Al, SiO_2 crystobalite and mullite crystallize.

Lanthanide-doped SiO_2–Al_2O_3 glasses were synthesized [34] from aerogels. Silicon and aluminium alkoxide precursors were hydrolyzed separately and then mixed with the lanthanide precursors: Pr (NO_3), Sm(NO_3), $EuCl_3$, at around 1,250 °C, the doped aerogels densified. However the authors [34] reported variations in the aluminium and lantahnide composition between the surface and the center of the densified materials .

In the process used to produce composite glasses, advantage is taken of the completely open pore structure of the aerogel to allow the migration of the liquid species (salt in solution) throughout the entire volume of the aerogel. The liquid phase is then eliminated, and the porous composite (aerogel + salt) is fully sintered, resulting in the synthesis of a multicomponent material (Figure 29.3). The porous structure of the aerogel is used as a volume host. The open porosity of a glass has already been used to modify the nature of material in the production of "Vycor" glass [35]. Xerogels are another matrix that enables the production of nanocomposites [36], but in this case, the open porosity is well below that possible using aerogels.

Given the small size of aerogel pores, one would expect to be able to prepare a nanocomposite using a very simple process. The size of second phase domains depends

on the size of the aerogel pores and on the concentration of salt in the liquid. This process has already been used to store nuclear wastes (fig. 6).

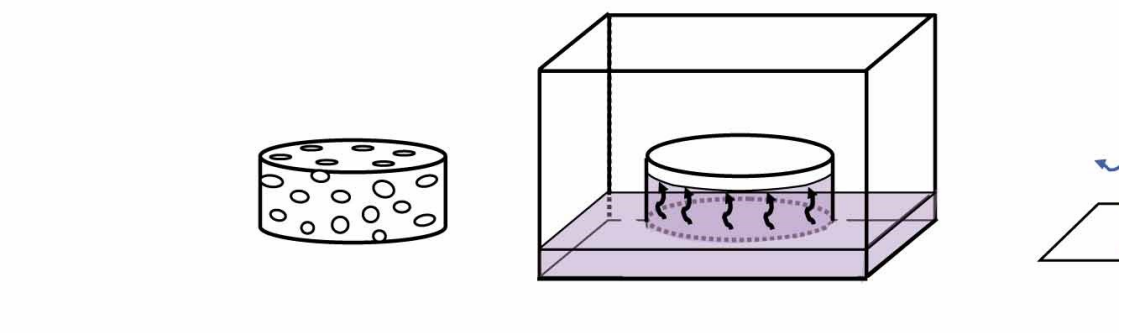

Figure 6. Steps of the containment process

4.4 Synthesis of silica aerogel host materials

In the proposed containment process, the large pore volume is used as a sponge to incorporate chemical species with the aim of obtaining a two phase material. However, the drawback of this porosity is poor mechanical properties that result in the cracking of unmodified aerogels during filling. Another important parameter is permeability. High permeability is generally an advantage because it means that the fluid and hence the chemical species of interest migrate easily into the porous network and lead to homogeneous distribution of the chemical species. However, due to the large microporosity, the permeability of standard aerogels is poor, typically a few nm^2 [4, 37]. Consequently, impregnation can take a long time. The permeability of the aerogel can be estimated from the *Carman–Kozeny equation* applied to a gel [40], an approximation that links permeability to pore size and can be written as:

$$D = (1-\rho_r) r_w^{\,2} / 4K_w \qquad (3)$$

where ρ_r is the *relative density*, r_w is the hydraulic radius (characteristic pore size), and K_w is the so-called *Kozeny constant*. However, in the case of gels, K_w is a function of ρ_r [25]. Over the range of density used in this study, it can be approximated by:

$$K_w = 2.03 + 2.56\rho_r, \quad 0.08 \le \rho_r \le 0.4. \qquad (4)$$

To sum up, the mechanical properties and permeability are the most important parameters for the loading process.

4.4.1. Partially sintered aerogels

One way to control the mechanical properties is to perform partial sintering. Depending on the duration of the heat treatment, microporosity is progressively

eliminated and partially sintered samples can be obtained with relative densities ranging from 0.15 (standard aerogel) and 1 (silica glass). Sintering has several effects: it increases connectivity and mechanical strength and collapses the small pores. In this way, sintering improves the ability of the porous network to resist the liquid filling step. However, the permeability *D* decreases with sintering [4,37]. A compromise is thus required in *relative density*, which should be high enough to obtain a matrix with acceptable mechanical properties but not too high, to still be sufficiently permeable. This compromise corresponds to a *relative density* in the range of 0.4–0.5 [6].

Figure 7 shows a lanthanide silica glass synthesized from a partially sintered aerogel.

Figure 7 lanthanide silica glass from a partially sintered aerogel

4.4.2. Nanocomposite aerogels

It is generally accepted that including particles or fibers in the material improves the mechanical properties. It is thus possible to adjust the apparent density, the mechanical property, and the permeability by adding silica powder (silica soot, such as aerosil) in the monomer solution, just before gelling [38, 39]. The mechanical properties rapidly increase with an increase in the percentage of silica powder [38] and a composite aerogel with a *relative density* close to 0.18 is able to resist the capillary stresses caused by the filling of the pores by an aqueous solution. Permeability increases with the addition of silica powder because the structure of the composite aerogel differs from that of the standard aerogel network. In the composite aerogel, gelling results from silica soot particles (40 nm diameter) sticking together. The natural spaces between them form larger pores and improve permeability.

The permeability of the composite aerogel is roughly 60 times higher than that of the sintered aerogel (Table 2).

Table 2. Relative density (ρ_r), mean pore size, and calculated permeability of a partially sintered aerogel and a composite aerogel

Kind of aerogel	ρ_r	r_w (nm)	D (nm^2)
Partially sintered aerogel	0.45	≈10	≈4.5
Composite aerogel	0.18	≈60	≈290

This new kind of nanocomposite aerogel is more appropriate for use as host matrix because of its improved mechanical properties and permeability.

4.5. Synthesis of loaded aerogels

The impregnation of these peculiar aerogels is used to trap chemical species in a silica matrix. After a soaking treatment, the host matrix is dried, then sintered. The resulting material is a nanocomposite comprised of oxide crystals embedded in a silica matrix.

As an example, cerium and neodymium nitrates are dissolved in water and after soaking, the samples are dried and heat treated in such a way to complete the drying and to decompose the nitrates. Further heating at ~1,100 °C fully sinters the silica network by viscous flow [6, 14].

The dense solids consist of a silica matrix in which oxides are trapped. Weight differences before soaking and after sintering make it possible to measure the loading in percentage weight. Figure 8 clearly shows that neodymium and cerium oxide loading increases with the concentration of the nitrate solution, and can reach 20%.

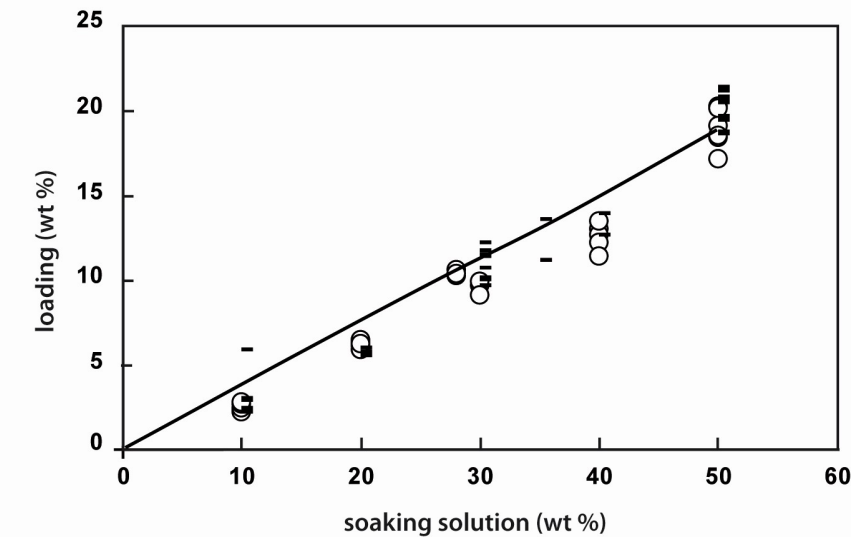

Figure 8. Changes in the loading rate versus the concentration of Nd (open circle) and Ce (dash) in the soaking solution.

4.6. Influence of loading on the sintering procedure

It should be noted that the final sintering procedure is affected by the loading solution. Figure 9 shows the dilatometer curves measured on the samples loaded with 13% of Nd_2O_3 and CeO_2. The dilatometer response, which expresses the sintering shrinkage ($\Delta L/L_0$ %), shows that loading increases the temperature range in which the shrinkage is maximized by up to 100 °C. The maximum shrinkage temperature is close to 1,150 °C for the native silica aerogel composite and close to 1,200 °C for silica aerogel containing Nd_2O_3. Loading with oxides hinders sintering because, in the case of amorphous materials, the crystalline phases (CeO_2 and Nd_2O_3) do not play an active role in the viscous flow mechanism responsible for sintering. The effect on the sintering rate is more pronounced in the case of Nd because of the more complicated structure of the glass ceramic, which contains vitreous silica and Nd_2O_3, but can also contain neodymium silicate and disilicate (see Sect. 5.4.). Consequently, the sintering step has to be adapted to the composition of the loaded porous glass and can vary by 50–100 °C.

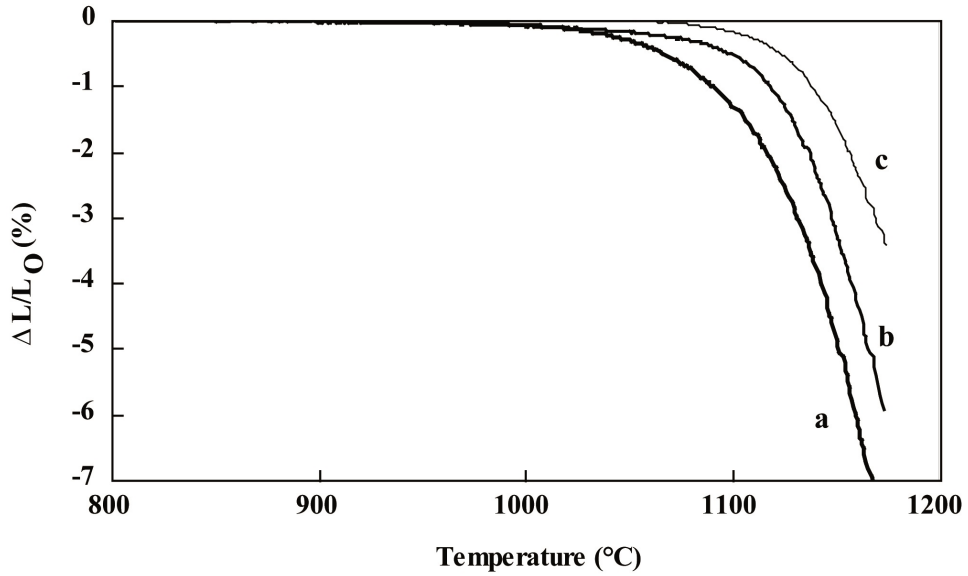

Figure 9. Shrinkage ($\Delta L/L_0$ %) of composite aerogel during sintering. **a:** SiO_2 (without loading) **b:** SiO_2+13% CeO_2. **c:** SiO_2+13% Nd_2O_3.

5. Examples of applications

We now describe three different studies that successfully demonstrated the concept of aerogel as a host matrix. The first concerns doped glasses exhibiting a Faraday effect, the second is related to polymorphism of thermotropic liquid crystals in confined media. In the third example, we provide a detailed explanation of the containment of nuclear waste in silica glasses derived from aerogels.

5.1. Faraday effect in aerogel-derived doped glasses

The Faraday effect is the phenomenon describing the modification, under a magnetic field, of the plane of polarization of light, by transparent substances. The angle of rotation θ depends on the nature of the substance and is proportional to the magnetic field (H) and to the length (l) of the sample. The Verdet constant (V) that characterizes the Faraday effect, can be calculated from the relationship:

$$V = f/l.\ H.\ \cos\theta \qquad (5)$$

where L is the length of the sample and θ is the angle between H and the direction of the propagation of the light.

To manufacture devices such as magnetic field probes or rapid optical switches, silica glasses containing rare earths are of great interest [41]. The proportion of rare earth makes it possible to adjust the Verdet constant. However, these systems have high melting temperatures and require treatment temperatures close to 1,800 °C. There are also problems of phase separation for certain compositions. All these experimental difficulties result in glasses of mediocre optical quality.

The gel-aerogel-glass process is another approach to synthesizing such binary lenses. To this end, alcogels doped with rare earth were synthesized by the use of erbium and dysprosium nitrates dissolved in a TEOS solution. However, because of the leaching effects during supercritical drying, the final concentrations were significantly lower than expected.

A possible way to avoid these uncontrolled leaching effects would be to use a aerogel partially densified as a host matrix. After partial sintering, the aerogel is soaked in a solution of rare earth nitrates and the final concentration can be controlled through the concentration of the nitrate solution and the pore volume.

After impregnation, the samples are heat treated at 600 °C to complete the drying and to decompose the nitrates. Doped glasses are obtained by an additional heat treatment at 1,100 °C. This method was successfully used to synthesize silica glasses doped with Er III and Mn II with a Verdet constant close to 3.5 [42, 43].

5.2. Containment of nuclear wastes in silica glasses

In the literature, the use of different materials has been considered to encapsulate high-level radioactive wastes [1–3]. These materials include glasses of various compositions, ceramics with a wide range of formulations, glass ceramic compounds, cements, and particles in metal matrices. Based on their production technology, the two best candidate materials are glasses and crystalline ceramics. Glass is a solid in which a wide range of waste can be dissolved and a number of countries have developed successful industrial-scale vitrification technologies to solidify their wastes. Glass can accept a wider range of wastes than ceramic and the processing feasibility has tended towards research into the development of borosilicate glass materials to immobilize waste solutes [1-3]. In this process, the radioactive elements are mixed and melted with a glass fritt (a borosilicate

glass containing sodium). This borosilicate nuclear glass has become the reference for the treatment of nuclear waste.

One of the main problems linked to the extended use of nuclear power is the fate of plutonium and actinides. Although there are a number of fission product radionuclides with high activity (^{137}Cs and ^{90}Sr) and a long half-life (^{99}Tc, 200,000 years; ^{129}I, 1.6×10^7 years) in spent nuclear fuel, actinides account for most of the radiotoxicity of nuclear waste because, after several hundred years, the radiotoxicity is dominated by ^{239}Pu (half-life = 24,100 years) and ^{237}Np (half-life = 2,000,000 years). Thus, most of the long-term risk is directly linked to the fate of these two actinides in the geosphere.

There are two basic strategies for the disposal of actinides: transmuting the actinides using nuclear reactors or accelerators or trapping them in chemically durable, radiation-resistant materials that are suitable for geological disposal. Therefore, researchers are investigating new containment matrices with high chemical durability, because it is important to limit the possible release of radionuclides if the matrix is destroyed by aqueous erosion.

In the case of oxide glasses, erosion starts in an initially dense glass with the extraction of ions that are highly mobile in the glass and are highly soluble in water, such as Na, Ca, or B. The erosion process leaves a skeleton whose chemical composition is essentially based on glass formers such as silica and alumina. High chemical durability is thus achieved through high silica content and low concentrations of oxide modifiers. What is more, silica glass offers good mechanical strength and resistance to thermal shock.

Thus, the use of “pure” silica glass optimizes the properties that characterize a suitable glassy matrix for the fixation of actinides, but preparing silica glass requires solving problems associated with high melting temperature (~1,800 °C). To ensure safe long-term storage, long-life nuclear wastes (actinides) must be incorporated in a matrix with excellent chemical durability. Among the usual glasses, silica glass, which does not contain alkali and boron, is expected to present high durability. Associated with good mechanical properties, low thermal expansion, and consequently good resistance to thermal shock, silica glass is a promising candidate. However, as mentioned above, preparation of the glass requires a high temperature (1,800 °C) melting process.

The use of porous silica aerogel as host matrix for the actinides has been proposed. For safety reasons the lanthanides, Ce and Nd, are used to simulate the III and IV valent actinides [47–48] [for example, Am(III), Cm(III), Np(IV), Pu(IV)]. Nd and Ce as actinides surrogates have also been chosen because of their dissimilar affinity for silica. Hence, Nd and Ce will lead to different kinds of glass ceramics, simulating the possible behaviors of the actinides in the presence of silica as a function of their affinity for silica. After drying, decomposition of the nitrates, and sintering, the glass ceramic material is obtained as described in paragraphs 4.5 and 4.6. (Figure 10)

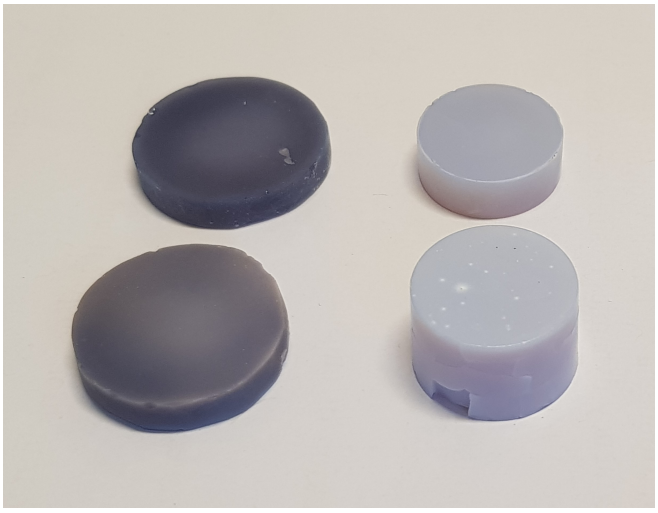

Figure 10. Glass ceramics loaded with cerium (left) and neodymium (rignt).

5.4. Characterization of glass ceramics

The final structure of the fully sintered materials achieved with this process is that of a composite material with surrogate loading as high as 20 wt%. The X-ray diffraction pattern (not shown) clearly demonstrates that the sintered Ce loaded material is a biphasic compound (SiO_2–CeO_2). On the other hand, the Nd-loaded sample shows three different crystalline phases, neodymium oxide (Nd_2O_3) but also neodymium mono (Nd_2SiO_5) and disilicate ($Nd_2Si_2O_7$) (Figure 11)

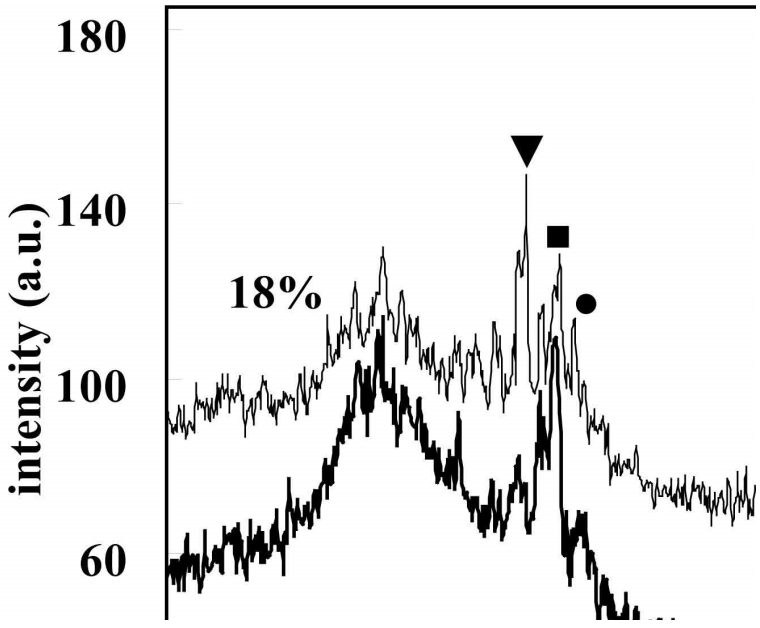

Figure 11. XRD of glass ceramics loaded with neodymium (10 and 18 wt%).

Changes in the X-ray patterns show that the structure of the crystalline phases is mainly Nd_2O_3 with a low loading percentage (2–10%) and tends towards $Nd_2Si_2O_7$ with concentrations higher than 14%. With less than 2% Nd loading, the sintered aerogel is amorphous leading to the conclusion that Nd associates with Si to form a neodymium silicate glass.

These structural differences are the result of the affinity of Ce and Nd ions for Si. In the case of Ce, the formation of a binary glass in a melting process is difficult, Ce(IV) generally forms crystalline CeO_2 [49,50]. Moreover, the crystalline phases of cerium silicates like $Ce_2Si_2O_7$ are not stable under 1,400 °C and are transformed into SiO_2 and CeO_2 [51, 52]. In the case of Nd, glasses with weight loading of between 2% and 5% have been obtained [53, 54]. The phase diagram also shows that, in addition to the oxide (Nd_2O_3), the different Nd silicates (Nd_2SiO_5 and $Nd_2Si_2O_7$) are stable at room temperature [55]. The size of the Ce and Nd domains ranges from 20–100 nm and increases with an increase in the loading percentage.

5. Aqueous erosion behavior

In the case of long-lived nuclear wastes, it is important to limit the possible release of actinides if the glass structure is destroyed due to alteration [56]. We have seen that the structure of Nd glass ceramics is more complicated than that of Ce glass ceramics. Because of these different structures, one can expect different resistance to aqueous corrosion. The chemical durability of the glass ceramics was measured with a conventional Soxhlet device consisting of a boiler containing ultra pure water and a condenser system. A sample monolith was placed in a recipient trough into which condensed steam was supplied in a continuous flow. The test was conducted at 100 °C,[57] and the sample analyzed after 28 days of leaching. The kinetics of glass corrosion were determined from analysis of the silica mass loss. The normalized silica loss $NL(SiO_2)$ characterizes destruction of the glass network by previous dissolution of the glass. $NL(SiO_2)$ (g/m^2) was calculated using the following formula:

$$\mathrm{NL}\left(\mathrm{SiO_2}\right) = \left(C\left(\mathrm{Si}\right) \times fc\right) / \left(\%\mathrm{SiO_2} \times S/V\right) \tag{6}$$

where C(Si) is the concentratoin of Si in solution (g/m^3), fc is oxide molar mass (fc = 2.139 for silica), $\%SiO_2$ is the mass fraction of SiO_2 in the glass ceramic, and S/V (m^{-1}) is the ratio of the glass surface (m^2) to the volume of the solution (m^3). As explained in the introduction, vitreous silica has high chemical durability. The mechanisms of alteration of the Nd and Ce loaded glass-ceramics with vitreous silica and standard nuclear borosilicate glass are now compared. For this study, we chose two glass ceramics loaded with 7 wt% of Nd_2O_3 and of CeO_2. Figure 29.10 shows the normalized loss of SiO_2 and the loss of surrogates measured on the two kinds of loaded material and on pure SiO_2.

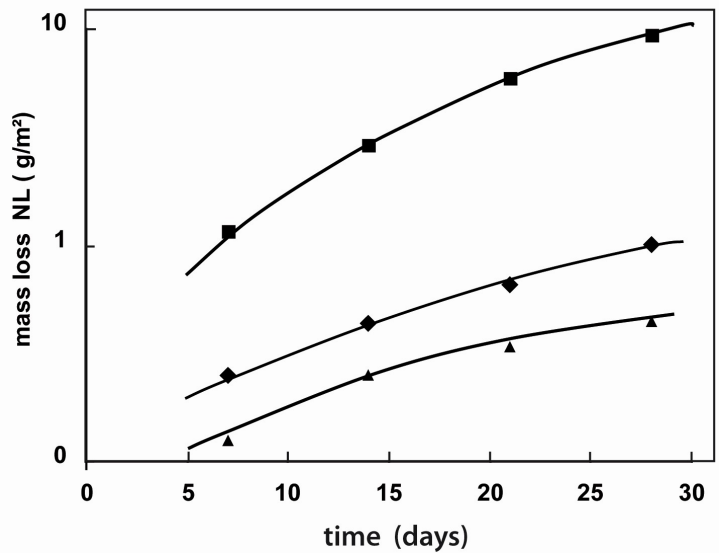

Figure 12. Normalized SiO_2 loss measured on two kinds of loaded material: Nd (squares), Ce (diamonds) and on vitreous SiO_2 (triangles) versus time.

From Figure 12, one can calculate the aqueous corrosion rate (V_0) for vitreous silica glass and for glass ceramics loaded with surrogate oxides. The corrosion rate (V_0) of pure silica is 0.015 g/m^2 per day, 100 times lower than the corrosion rate of the usual nuclear waste glasses in which V_0 is equal to 2 g/m^2 per day [57]. V_0 for the glass ceramics loaded with the Ce and Nd is, respectively, 0.035 g/m^2 per day and to 0.25 g/m^2 per day. This result is evidence for the improved chemical durability of glass ceramics compared to that of the standard glasses used to store nuclear waste. Thanks to its simple structure, the corrosion rate of Ce glass ceramics is quite close to that of the pure silica, the slight difference can be attributed to higher silica dissolution at the interface with the cerium oxide domain, corrosion could be activated by thermomechanical stresses. The corrosion rate of the Nd glass ceramic is 8 times higher than that of pure SiO_2. This result confirms the fact that part of the glass matrix is made of a neodymium silicate glass, which is less durable than SiO_2.

Because of their different degrees of affinity for silica, the two surrogates used, Nd and Ce, indicate what kind of behavior can be expected when actinides are able to form silicate phases or binary glasses or, on the contrary, when no silicate crystalline or glassy phases can exist. In the latter case, chemical durability is improved and is close to that of vitreous silica. In an open system, flowing groundwater in which solubility limits are not reached, the leach rate for silica and loaded glass-ceramics used in this comparison is two orders of magnitude lower than the leach rate of borosilicate glasses [58].

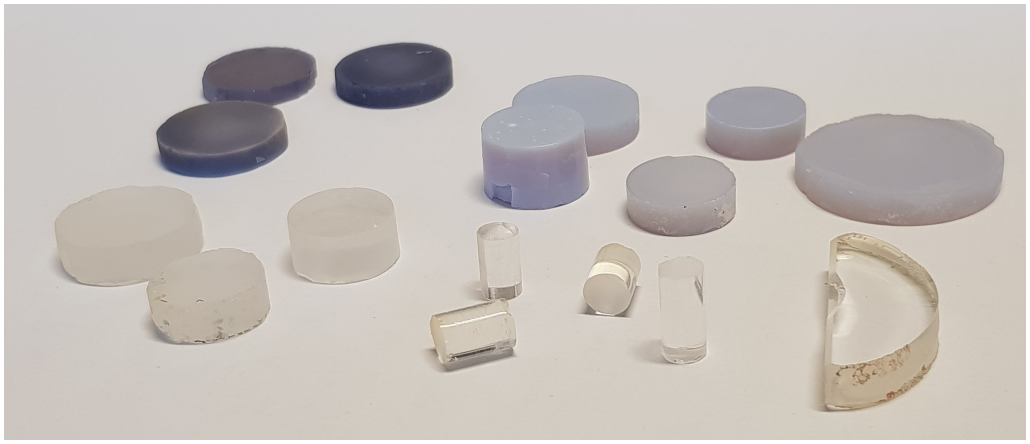

Figure 13. Different silica glasses and glass ceramics obtained using the gel-aerogel-glass-process

Recently, a mixed silica-silver aerogel was shown to be an effective absorber for radioactive iodine [59]. Its high adsorption capacity makes silica-silver aerogel (Ag0) an attractive choice for the containment of iodine compounds resulting from the reprocessing of nuclear fuel. After loading by iodine, the isostatic pressing (1,200 °C-207MPa) of the silica–silver aerogel allowed complete densification in a glass containing between 20 and 39 wt% of iodine encapsulated in a silica matrix. Iodine was retained in the form of nano-and micro-particles of AgI uniformly dispersed throughout the silica based-matrix

6. Conclusion

Aerogels are generally defined and synthesized as end materials but their use as precursors is an attractive alternative that offers new opportunities. A successful example is sintering silica aerogels to obtain pure silica glass [60,61. The possibility to use an ultraporous volume as a host matrix before sintering extends the potential applications of this method (Figure 13).

However, the properties that are required for a silica aerogel as a precursor are completely differerent from the properties used required of an aerogel. These are large pore volume and specific surface area, resulting in poor mechanical properties [62]. When an aerogel is used as a host matrix, the main objectives are to obtain high mechanical stability and a large mean pore size, both of which are the opposite of large pore volume and a high specific surface area. Consequently, aerogel hosts require a different synthetic process to achieve these objectives. In addition to the need for a new aerogel synthetic protocol, the influence of surface reactivity and of the pore structure on the physical and chemical properties of invading species is a research field that remains largely unexplored.

We have given one example in which the reactivity of the matrix-chemical species (in nuclear waste containment) strongly affects the physical properties of the final two phase materials. It should also be emphasized that this process enables the synthesis of multiphase materials that cannot be achieved using standard methods. For example, special glass ceramics could be synthesized in compositions that usually produce homogeneous glasses by the melting process. Sintering can preserve the heterogeneous structure in the glass matrix, which is not possible when the melting step dissolves and homogenizes the different chemical species. Numerous composite materials including metal–gel, polymer–gel, gel–gel could also be produced. In this chapter, we focused on a silica matrix but other kinds of oxides (alumina, zirconia, etc.) or organic aerogels can also be used. The advantage of the silica matrix compared to a ceramic or organic matrix is that it can be sintered by viscous flow after soaking, which entraps the doping species. Aerogel has specific properties innate to its expression as the lightest solid material ever synthesized. The ability to fill and/or sinter the porous structure is another way to extend the applications of aerogels in the future.

References

1 Jacquet-Francillon N, Bonniaud R, and Sombret C (1978) Glass a material for the final disposal of fission products. Radiochimica Acta 25: 231–240

2 Glasser FP (1985) The role of ceramics, cement and glass in the immobilization of radioactive wastes. Br. Ceram. Trans. J. 84: 1–8

3 Donald IW, Metcalfe BL, Taylor RNJ (1997) The immobilization of high level radioactive wastes using ceramics and glasses. J. Mat. Science 32:5851–5887

4 Brinker JF, Scherer GW (1990) Sol-Gel Science, Academic Press, N.Y.

5 Prassas M, Woignier T, Phalippou J (1990) Glasses from aerogels part 1 The synthesis of monolithic silica aerogel. J Mater Sci 24: 3111–3117

6 Woignier T, Phalippou J, and Prassas M (1990) Glasses from aerogels part 2: The aerogel glass transformation. J Mater Sci 25: 3118–3126.

7 Woignier T , J Phalippou J (2016) Glasses: Sol–Gel Methods in" Reference Module in Materials Science and Materials Engineering". Elsevier Inc doi:10.1016/B978-0-12-803581-8.02341-9;

8 Sempere R, Bourret D, Woignier T, Phalippou J, Jullien R (1993) Scaling theory and numerical applications of aerogel sintering. Phys Rev Lett 71: 3307–3312

9 Bourret A (1988) Low density silica aerogels observed by high resolution electron microscopy.Europhysics lett 6(8):731–737

10 Woignier T, Phalippou J, Pelous J, Courtens E (1990) Different kinds of fractal structures in Si02 aerogels. J Non-Cryst Solids 121:198–204

11 Woignier T, Fernandez Lorenzo C, Sauvajol JL, Schmidt JF, Phalippou J Sempere R (1995) Raman study of structural defects in SiO_2 aerogels. J Sol-Gel Sci and Techn 5:167–172

12 Frenkel J (1945) Viscous flow of crystalline bodies under action of surface tension. J. Phys. (Moscow**) 9(**5):385–391

13 Woignier T (1993) Le proceed " Sol-Gel-Verre" , Habilitation thesis, Montpellier

14 Scherer GW (1977), Sintering of low density glasses: I. Theory. J. Am. Ceram. Soc. 60 (5/6):236–239

15 Scherer GW (1991) Cell Models for Viscous Sintering. J. Am. Ceram. Soc. 74(7):1523–1531

16 Scherer GW, Calas S, Sempéré r (1998) Sintering Aerogels. J Sol-Gel Sci and Techn 13: 937–943

17 Emmerling A, Gerlach R , Goswin R, Gross J, Reichenauer G, Fricke J , Haubold HG(1991) Structural modifications of highly porous silica aerogels upon densification. .J. Appl. Cryst. 24: 781–787

18 Su SR, Onorato PIK (1996) in *Better Ceramics Through Chemistry II*, Mater. Res. Soc. Symp., Pittsburgh, PA, pp. 237– 244

19 Vacher R, Woignier T, Phalippou J, Pelous J, Courtens E (1989) On the fractal structure od f silica aerogels. Rev. Phys. Appl. 24(4): C4-127–C4-131

20 Schaefer DW , Olivier BJ, Ashley CS, Richter D , Farago B, Frick B, Hrubesh L, van Bommel MJ, Long G, Krueger S(1992) Structure and topology of silica aerogels. J. Non-Cryst. Solids 145:105–112

21 Jullien R, Olivi-Tran N, Hasmy A, Woignier T, Phalippou J, Bourret D, Sempéré R.(1995) Scaling theory and numerical applications of aerogel sintering. J Non Cryst Solids 188:1–10.

22 Zanotto ED (1992) The formation of unusual glasses by sol-gel processing. J Non-Cryst Solids 147&148: 820–823

23 Prassas M, Phalippou J, Zarzycki J. Sintering of monolithic silica aerogels. In: Hench LL, Ulrich DR, editors. Science of ceramic chemical processing, vol. 17. New York: Wiley; 1986.p. 156–67.

24 Jensen KI, Schultz JM, , Kristiansen FH (2004) Development of Windows Based on Highly Insulating Aerogel Glazings. J. Non-Cryst. Solids 350 : 351-357

25 GaoaT, Jelleb BP, Gustavsena A, Hed J (2015) Synthesis and characterization of aerogel glass materials for window glazing applications *Advances in Bioceramics and Porous Ceramics VII.* Edited by Roger Narayan and Paolo Colombo Copyright © 2015 The American Ceramic Society. P 142-150

26 . Esquivias L, Zarzycki J (1988) in *Ultrastructure Processing of Advanced Ceramics,* edited by J.D. Mackenzie and D.R. Ulrich (Wiley, New York,) p. 255-270

27 Lee K-H, Koh Y-P, Lim J-G (1994) Synthesis of Silica **g**lass Using Solventless Sol-Gel Process J Sol-Gel Sci and Techn. 2:907-912

28 Woignier T, Phalippou J, Zarzycki J Monolithic aerogels in the systems SiO_2-B_2O_3, SiO_2-P_2O_5, SiO_2-B_2O_3-P_2O_5 (1984) J Non-Cryst Solids 63(1,2):117-130

29 Woignier T, Phalippou J (1986) Binary glasses from aerogel, First International Workshop on Non-Crystalline solids, Current topics on Non-Crystalline Solids, M.D. BARO, N. CLAVAGUERA ed., World Scientific p 415-422.

30 Vestreghem H, Fargeot D,. DaugerA (1989) Sintering of monolithic cordierite aerogels Rev. Phys. Appl. 24(4):C4-65-C4-70 DOI: 10.1051/jphyscol:1989411

31.Bouaziz J, WoignierT, Bourret D, Sempere R (1986) Diffusion phenomena in partially densified silica gels and doped silica glasses elaboration, J Non Cryst Solids, 82, (1986) 225-231

32 Ramírez-Del-Solar M, De la Rosa-Fox N, Esquivias L, Zarzycki J (1990) Effect of the method of preparation on the texture of TiO_2- SiO_2 gels, 121(1–3): 84-89

33 Fujiyama T, Yokoyama T, Hori M, Sasaki M (1991)Silica glass doped with Nd and Al prepared by sol-gel method. Change in the state of aluminium in the formation process. J Non Cryst Solids 135(2–3) :198-203

34 Grandi S, Costa L (1998), Lanthanide-doped SiO_2–Al_2O_3 aerogels and densified glasses. J Non Cryst Solids 225: 141-145

35 Simmons JH, Macedo P B, Barkatt A, Litovitz TA (1979) Fixation of radioactive waste in high silica glasses. Nature 278: 725–731

36 Aravind PR, Shajesh P, Mukundan P, Pillai K, Warrier KGK (2008) Non-supercritically dried silica–silica composite aerogel and its possible application for confining simulated nuclear wastes. J Sol-Gel Sci Technol 46: 146- 152 https://doi.org/10.1007/s10971-008-1714-

37 Reynes J, Woignier T, Phalippou J (2001) Permeability measurements in composites aerogels: application to nuclear waste storage. J Non-Cryst Solids 285: 323–327

38 Toki M, Miyashita S, Takeuchi T, Kande S, Kochi A (1988) A large-size silica glass produced by a new sol-gel process. J Non-Cryst Solids 100: 479–482

39 Marlière C, Woignier T, Dieudonné P, Primera J, Lamy M, Phalippou J (2001) Two fractal structure in aerogel. J Non-Cryst Solids 285:175–181

40 25. Scherer GW (1994) Hydraulic Radius and Mesh Size of Gels J Sol-Gel Sci and Techn 1: 285–291

41 Massey GA, Erikson DC, Kadtec RA (1975) Electromagnetic field components: their measurement using linear electrooptic and magnetooptic effects**.** Appl. Opt.14:2712-2719

42 Sempere R, Bourret D, Bouaziz J, Sivade A,(1989) Faraday effect in doped aerogels , Rev. Phys. Appl. 24(4): C4 227- C4231

43 Bouaziz J, Sempere R, Bourret D, Regnier J(1986) Faraday effect of sol gel derived glasses. J. Non-Cryst. Solids 82:183-189

44 Iannachione G, Crawford G, Zumer S, Doane J, Finotello D (1993) Randomly constrained orientational order in porous glass .Phys. Rev Lett. 71 :2595-2598

45 Bellini T, Clark N, Muzny C, Wu L, Garland C, Schaeffer DW, Oliver B (1992) Phase behavior of the liquid crystal 8CB in a silica aerogel Phys. Rev. E 51:788-791

46 Fehr C, Dieudonne P, Primera J, Woignier T, Sauvajol JL, Anglaret E (2003), Solid state polymorphism of liquid crystals in confined geometries. Eur. Phys. J. E 12: 13-16.

47 Lopez C, Deschanel X, Auver CD, Cachia JN, Peuget S, Bart JM, (2005) X-ray absorption studies of borosilicate glasses containing dissolved actinides or surrogates. Phys. Scr 115: 342–345

48 Advocat T, Fillet C, Marillet J, Leturcq G, Boubals JM, Bonnetier A, (1997) Nd-Doped Zirconolite Ceramic and Glass Ceramic Synthesized by Melting and Controlled Cooling, in Scientific Basis for Nuclear Waste Management XXI, edited by Ian G. McKinley. Charles McCombie (Mater. Res. Soc. Symp. Proc. 506:55–62 Warrendale, PA

49 Lopez C, Deschanel X, Auver CD, Cachia JN, Peuget S, Bart JM, (2005) X-ray absorption studies of borosilicate glasses containing dissolved actinides or surrogates. Phys. Scr 115: 342–345

50 Haire RG, Assefa Z, Stump N (1998) Fundamental science of elements in selected immobilization glasses: Significance for TRU disposal schemes." Mat Res Soc Symp Proc V 506: 153–160

51 Felsche J, Hirsiger W (1969) The polymorphs of the rare earth pyrosilicates RE, Si, O, [RE: La, Ce, Pr, Nd, Sm]. J Less-Common Met 18: 131–37

52 Van Hal H A M, Hintzen H T (1992) Compound formation in the Ce2O3-SiO2 system. J of Alloys and Compounds 179: 77–85

53 Thomas I M, Payne S A, Wilke G D (1992) Optical properties and laser demonstration of Nd-doped sol-gel silica glasses. J Non-Cryst Solids 151:183–190

54 Pope EA, Mackenzie JD (1993) Sol gel processing of Neodymia –silica glass. J Am Ceram Soc. 76(5): 1325–1329

55 Miller RO, Rase DE (1964) Phase equilibrium in the system Nd_2O_3-SiO_2. J Am Ceram Soc 47(12): 65–654

56 Lutze W, Malow G, Ewing R C, Jercinovic M J, Keil K (1985) Alteration of basalt glasses: implications for modelling the long-term stability of nuclear waste glasses. Nature 314: 252–255

57 Ji H, Rouxel T, Abdelouas A, Grambow B, Jollivet P (2005) Mechanical behaviour of a borosilicate glass under aqueous corrosion. J Am Ceram Soc 88 (11):3256–325

58 Woignier T, Calas S, Reynes J (2011) From Nano composites aerogels to glass ceramics.Solid State Phenomena 172-173: 791-796

59 Matyáš J , Canfield N, Sulaiman S , Zumhoff M (2016) Silica-based waste form for immobilization of iodine from reprocessing plant off-gas streams. J. Nucl. Mater. 476 : 255-261 https://doi.org/10.1016/j.jnucmat.2016.04.047

60 Woignier T, Duffours L (2018) Densification and strengthening of aerogels by sintering heat treatments or plastic compression. Gels 4, 12-20 doi 10.3390/gels4010012

61 Woignier T , Prassas M, Duffours L (2019) Sintering of aerogels for glass synthesis. Accepted in J Sol-Gel Sci Technol .

62 Woignier T , Primera J, Alaoui A, Etienne P , Despetis F, Calas-Etienne S (2015) Mechanical Properties and Brittle Behavior of Silica Aerogels. Gels , 1, 256-275 doi:10.3390/gels1020256